Compliant Electric Actuators Based on Handed Shearing Auxetics

Lillian Chin, Jeffrey Lipton, Robert MacCurdy, John Romanishin, Chetan Sharma, and Daniela Rus

***Abstract*— In this paper, we explore a new class of electric motor-driven compliant actuators based on handed shearing auxetic cylinders. This technique combines the benefits of compliant bodies from soft robotic actuators with the simplicity of direct coupling to electric motors. We demonstrate the effectiveness of this technique by creating linear actuators, a four degree-of-freedom robotic platform, and a soft robotic gripper. We compare the soft robotic gripper against a state of the art pneumatic soft gripper, finding similar grasping performance in a significantly smaller and more energy-efficient package.**

I. INTRODUCTION

Compliance is the fundamental advantage of soft robotics. By being able to deform their entire structure in response to loading, soft robots demonstrate significantly better safety, robustness and grip performance than rigid robots [1]. Although compliant rigid-bodied mechanisms existed before the development of soft robotics – such as impedance-matching based control schemes [2] and series elastic actuators [3] – soft robots' continuously deformable bodies are a simpler low-cost solution to introducing compliance.

Fluid driven actuators, specifically pneumatic [4, 5], vacuum [5, 6] and hydraulic [5, 7] actuators, are the most common approaches for creating compliant soft robots [1, 8]. The pneunet actuators were among the first developed for soft robotics [1]. They are relatively simple to fabricate, have high strength to weight ratios, and are deformable across their length [9]. However, since most control and power systems are electric, all fluid-driven actuators require compressors, pumps and valves to convert electric power and signals to fluid flows [10]. This adds physical bulk and generates power inefficiencies [11]. Additionally, fluid-based actuators suffer significant failures when punctured, limiting use outside the lab or factory environment. Efforts have been made to address these problems, such as creating puncture resistance by embedding fibers [12] or creating more efficient pneumatic-electric transducers [13]. However, there remains a clear need for robust and compliant robotic actuation that efficiently converts electricity to actuation. To address these issues, we propose using handed shearing auxetics (HSA) as a compliant actuation scheme. Unlike other soft actuators, HSA cylinders directly couple twists into the linear extension of a continuous medium. This allows torques from a standard electric motor to be translated directly into linear extensions. These HSA actuators do not need to contain a fluid or vacuum, so punctures do not cause system failures. Constraints on HSA cylinders can convert extension into bending just as they do for pneunet actuators [4] and fiber reinforced actuators [15], allowing us to address many soft robotic needs with these basic ingredients of linear extension and bending.

All researchers are with the Computer Science and Artificial Intelligence Lab at the Massachusetts Institute of Technology, 32 Vassar St, Cambridge, MA 02139, USA. {ltchin, jlipton, maccurdy, johnrom, ban, rus} @ csail.mit.edu

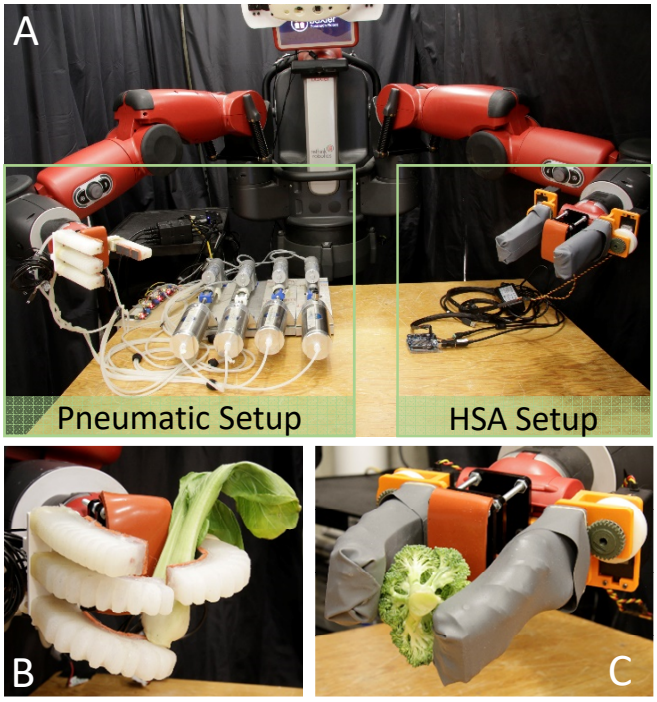

Fig. 1. (A) Overview of grasping test setup and actuators required for each soft hand. Note the large off-board pneumatic pistons and four power supplies required to actuate the pneumatic hand (B) compared to the on-board servo for the electrically-actuated handed-shearing auxetic hand (C). The actuation scheme for the pneumatic hand comes directly from [14]

We explain how we adapt HSAs for robotic application by creating cylinders patterned to have HSA properties. By combining sets of differently-handed HSA cylinders, we create a linear actuator that can extend by 60% of its initial length, and a 4 degree-of-freedom (DOF) robotic platform that can pitch and roll by 100°, yaw by 280°. Finally, we adapt the HSA pattern to create a soft robotic gripper, which we compare against a state-of-the art pneumatically-actuated soft gripper [14]. We found that our HSA system has comparable grasping performance to the pneumatic system; both grasp 72% of the objects in our test set, but the HSA actuators are significantly more space and energy efficient. Overall, the HSA actuators have compliance similar to standard pneumatic actuators, but with simpler construction, greater puncture resistance, and easier integration with ex-

isting robotic systems.

In this paper we:

- demonstrate and characterize actuators created by twisting HSA cylinders
- illustrate how constraints on HSA cylinders can produce bending actuators
- develop a gripper based on HSA actuators and compare it to state-of-the-art soft pneumatic grippers

II. BACKGROUND

A. Motor Driven Actuation for Soft Robots

While there are many materials that can directly convert electricity into movement, motors are still the most versatile, cost effective, and efficient means of doing so for robots. Compliant motor-driven transmissions generally fall into the categories of cable-driven tendons or series elastic actuators (SEAs). Although complex systems such as [16] and [17] have successfully used cable tendon methods, the design and fabrication of cable-driven systems remains highly complex. Since cables require tension, these tendon systems require significant infrastructure, such as rigid pulleys, sheathing, and spindles [18]. Also, a single failure in the transmission line can disable an entire limb, giving cable-based systems similar robustness issues as pneumatic systems. By contrast, SEA systems are much more robust [19], as their elastic elements act as low pass filters for shocks and impacts [3]. However, deformation is restricted to just the joints, so the body of the robot remains rigid, negating many of the benefits that soft robotic systems offer [19].

B. Handed Shearing Auxetics

Auxetic materials are defined by the material's perpendicular expansion under tension loads, i.e. having a negative Poisson's ratio [20]. The auxetic property emerges from periodic patterns of links and joints [21] within the material. While some materials have these patterns at the level of chemical bonds [22, 23], most derive the auxetic property from patterns formed in a bulk material [24].

Auxetic patterns are periodic; a single unit cell is repeated to fill 3D space or tile 2D surfaces. The movement of the links of a single unit cell and the pattern as a whole is driven by an angle (θ) between two links. As θ varies, the areas of all of the unit cells expand or contract together. Some auxetic patterns couple a global shearing with this expansion [25]. For these shearing auxetic materials, the area of the unit cell increases as the unit cell itself shears. Because each unit cell is shearing in the same direction, these materials have a net shear.

Since a net shear on the surface of a cylinder is the same as twisting the cylinder, a shearing auxetic cylinder would expand when twisted. Unhanded shearing auxetics are symmetric around their point of maximum extension, allowing an unhanded shearing auxetic cylinder to switch between twisting to the left and twisting to the right. We recently discovered a framework for generating handedness in two-dimensional shearing auxetics [26]. These HSA patterns shear only towards the right or only towards the left when expanding and are unable to switch between chiralities (ex. Fig. 2A). This yields stable left or right-handed chiral structures which can then be used as the basis for further mechanical designs.

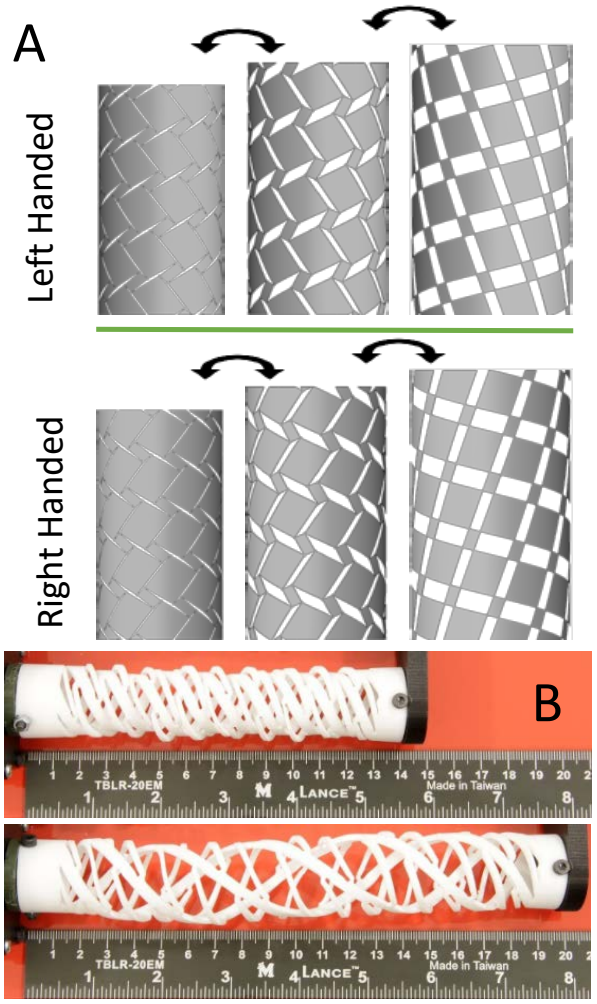

Fig. 2. (A) Handed shearing auxetic (HSA) cylinders come in left and right handed pairs, depending on what is patterned around the cylinder. (B) Demonstration of HSA cylinders extending through twisting

III. DESIGN OF HANDED SHEARING AUXETIC ACTUATOR

Since HSAs have stable chiralities, pairs of HSA cylinders with opposite chiralities can be paired together and enable various robotic applications. Both HSA cylinders and unhanded shearing auxetic cylinders convert a twist to change in length, but the HSA's fixed relation between twist direction and expansion makes it easier to create actuators from HSA cylinders.

To twist a cylinder, we need to apply opposite torques to each end of the cylinder. Since right and left HSAs are chiral to one another, when both ends are connected, the cylinders will directly oppose the other's twisting tendencies and create a self-locking structure. From this, we immediately see how we can create a linear actuator. An HSA pair by itself is

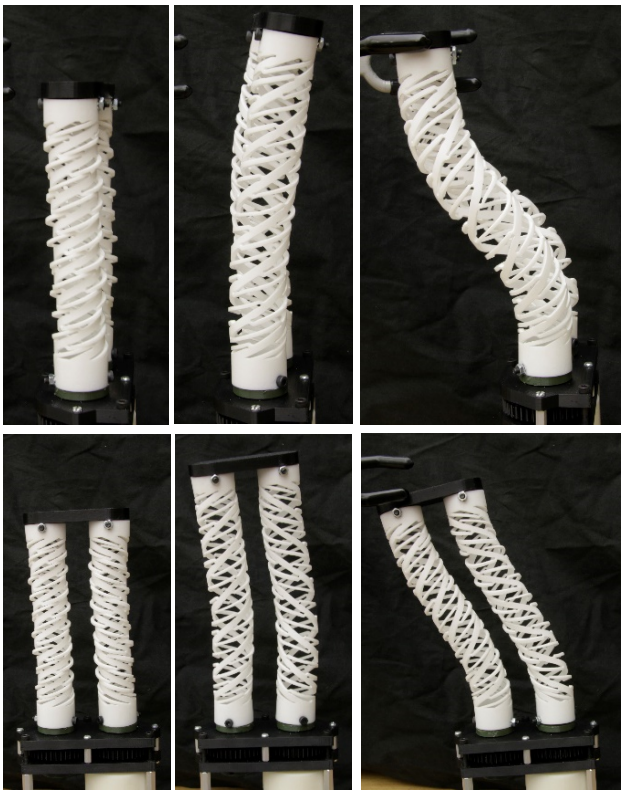

Fig. 3. Demonstration of a linear actuator created by a pair of handed shearing auxetic cylinders (HSA). Linear extension and compression is achieved just by the use of a single servo. Compliance is created due to the flexible nature of the PTFE tube that the HSA is patterned into.

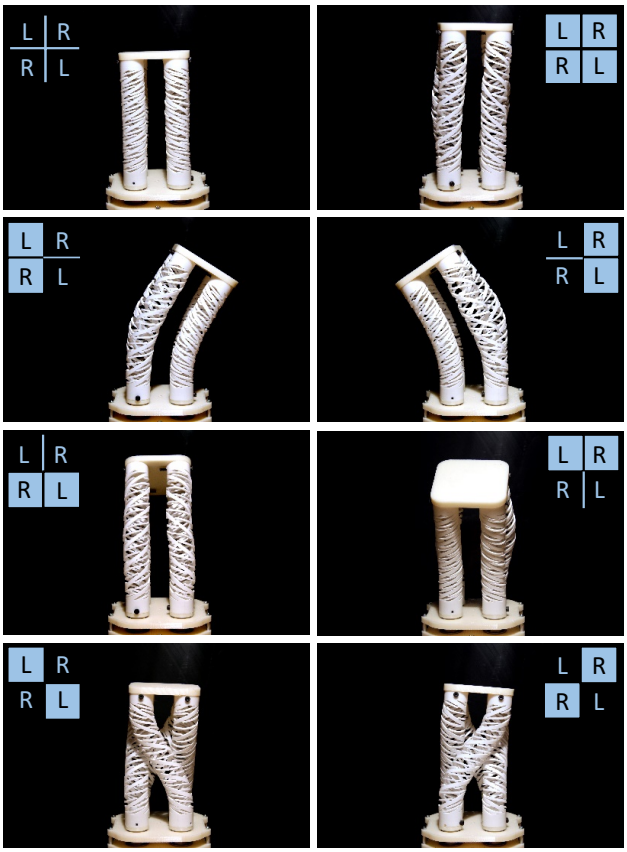

Fig. 4. Demonstration of a 4-degree-of-freedom robotic platform created by two left-handed and two right-handed shearing auxetic cylinders (HSAs). By actuating different sets of HSA cylinders, the platform is able to extend and twist. Going down each row from top to bottom, we see extension in the y axis and rotation about the x, z, and y axes, respectively.

a direct analogue to a compliant linear actuator. When we rigidly connect one end of an HSA pair together, the HSA cylinders apply counter torques to each other, creating a ”locked end”. By applying counter torques on the other end (the ”actuation end”), the system extends. The simplest way to ensure counter torques on the free ends is to connect them together with gears as seen in Figure 3B. Turning the gears applies opposite torques and rotational displacements to the HSA, causing the structure expands. If the HSA cylinders are made out of a deformable material, the structure will bend and buckle under external loading, demonstrating compliance.

We can extend this concept further by noting that we can create external loading through another HSA pair. By directly connecting two HSA pairs together, a 2-DOF actuator is created. Actuating one pair causes the structure to bend towards the other, and actuating both causes it to extend.

Expanding this concept further, if we alternate left and right-handed HSA cylinders in a 2x2 grid and actuate each cylinder independently, we can create a 4-DOF actuator. As each side of the 2x2 grid activates, the structure bends away from the activated side (Figure 4). Simultaneously activating both right or both left handed cylinders generates a net torque on the far end of the structure, causing it to twist.

IV. CHARACTERIZATION OF HANDED SHEARING AUXETIC ACTUATOR

Since all of our actuators are based on combining several HSA cylinders, characterizing a single HSA cylinder provides the analytical foundation to understand compositions of actuators. We proceed by characterizing a single HSA cylinder through a hysteresis test to obtain a baseline elastic stiffness and rotational compliance. We then use this analysis to inform our evaluation of the linear actuator and 4-DOF robotic platform's full range of motion. Results are summarized in Table I. Axes are defined as described in Fib. 4.

Each HSA cylinder is based on 25.6 mm diameter PTFE tubes with a 1.58 mm wall-thickness. The pattern we use is closely related to the fiber network described in [27]. We tessellated our pattern so that there were only three base units around the circumference. The pattern was then laser cut into the PTFE tube via a rotary engraving attachment on a Universal 120W laser cutter. For the linear actuator and 4-DOF robotic platform, each tube was then bolted into 3D printed caps to pair the left-handed and right-handed HSA cylinders together and driven by multi-turn HS-785 HB servos controlled through an Arduino.

We performed a hysteresis test by cyclically pulling a

TABLE I
MECHANICAL PROPERTIES OF HANDED SHEARING AUXETICS

HSA Cylinder (Fig. 2B)	
System Weight	30.8 g
Stiffness, no rotation	285 ± 0.7 N/m
Stiffness, allowing rotation	193 ± 0.3 N/m
Linear Actuator (Fig. 3)	
System Weight	351 g (w. servos)
Max Extended Length (in y)	217 ± 7.8 mm
Min Extended Length (in y)	144 ± 0.4 mm
Robotic Platform (Fig. 4)	
System Weight	925 g (w. servos)
Max Extended Length (in y)	238 ± 0.5 mm
Min Extended Length (in y)	148 ± 0.1 mm
Max Rotation about x	45 ± 4.2°
Min Rotation about x	-54 ± 2.5°
Max Rotation about z	53 ± 2.6°
Min Rotation about z	-52 ± 0.86°
Max Rotation about y	144 ± 27°
Min Rotation about y	-138 ± 11°

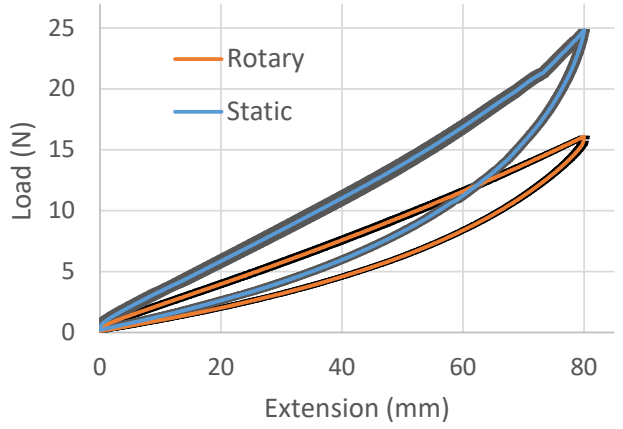

Fig. 5. The cyclic loading of a single handed shearing auxetic cylinder with and without allowing rotation at the ends. Note the lower stiffness when rotation is allowed (285 ± 0.7 N/m vs. 193 ± 0.3 N/m)

92 mm long HSA cylinder to 80 mm extension at a rate of 50 mm/min 3 times. We performed this test both with and without the ability of the base to rotate. The results are seen in Figure 5. In tension, the freely rotating HSA has a stiffness of $200 \pm 2\ N/m$ while the static HSA has a stiffness of $291 \pm 2\ N/m$. The lower stiffness when rotational motion is allowed is reflective of HSAs extension from twisting. From this hysteresis curve, we see that when an HSA is held at a specific position by a motor, it will act as an elastic element, allowing additional loading to deform the structure. By controlling the rotation of the HSA cylinders ends, we can control the effective stiffness of the HSA cylinder. Note that the hysteresis curve also demonstrates that the HSA system will lose energy in each actuation cycle.

To quantify the maximum range of the linear actuator and 4-DOF platform, we used an OptiTrack motion capture system to track the top and bottom plane of the system, while manually driving each of the servos to achieve system limits. Maximum linear extension/compression in the y axis was achieved by driving the servos until the internal living hinges were extended or compressed fully. Similarly, maximum rotation capabilities for the robotic platform were determined by fully compressing or extending the appropriate pair of HSA cylinders as highlighted in Fig. 4 to generate bending until no more rotation could be achieved.

Since the compliance of each HSA cylinder changed upon elongation / compression, it became tricky to ensure a precise and consistent curve for the rotation measurements, making it a bit unclear whether these values were actually the maximum achieveable range. This may explain the deviation between rotations about x and z, when by symmetry, we would expect a somewhat more consistent rotation range as well as the high variance for rotations about y. Nevertheless, given the manual control scheme, both the linear actuator and robotic platform demonstrated an impressive control volume and orientation.

V. DESIGN OF SOFT GRIPPER

In the previous sections, we demonstrated how HSA cylinders can be used to make linear extension and how composing HSA cylinders can generate bending. In this section, we show how adding constraints to an HSA cylinder can directly convert an HSA pair into a bending actuator, which we use to make a compliant gripper.

Pneunet actuators, like those described in [4], use a strain limiting layer to convert linear extension into a bending motion. However, using a bonded strain limiting layer is not possible for our HSA approach. Since the cylinders counter-rotate, a bonded strain limiting layer would deform and be sheared from the surface. Instead, we add strain limiting in a similar manner to fiber reinforced pneumatic actuators [15]. Embedded fiber networks have been shown to convert a single pressure input into complex motion [15]. Similarly, if we create internal constraints in the HSA pattern, we can create the desired bending motion.

To create the internal constraints, we added a connecting line through the HSA cylinder to bond neighboring HSA unit cells (Fig. 6A). The line was parallel to the diagonal of the HSA unit cell and was staggered to avoid constraining the living hinge joints needed for the auxetic pattern to function. These constraints were mirrored between the left and right HSA cylinders (Fig. 6B,D). As the cylinders rotate, the constrained HSA pair bends, and the constraints rotate to become the inner radius of the curved pair (Fig. 6C,E).

We then used these constrained HSA pairs as fingers for a soft robotic hand. By mounting two constrained HSA pairs opposite one another, we created a compliant two-finger HSA hand. To enable direct comparison to state-of-the-art pneumatic grippers such as [14], we modified our

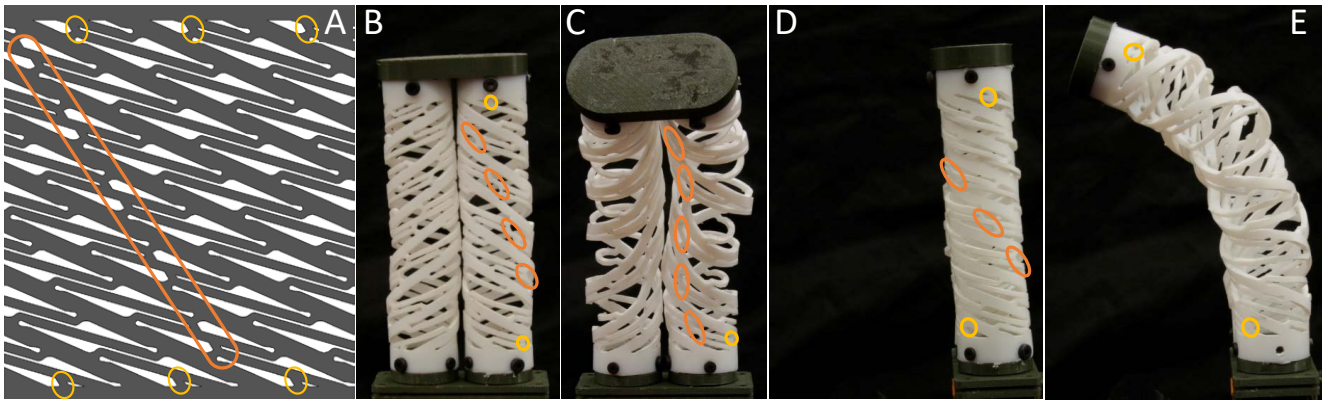

Fig. 6. Handed shearing auxetic (HSA) pairs bend if properly constrained. The main constraints are highlighted in orange, and boundary conditions are marked with yellow highlights. (A) The constrained pattern that is cut into HSA cylinders via laser cutter. When unactuated (B, D), the main constraints form a line on the surface connecting adjacent cells. When bent (C, E), the main constraints form the inner radius of the bent HSA.

linear actuator design to fit the geometry of the hand for Rethink Robotic's Baxter robot, moving the servo to the side of the fingers (Fig. 7). We also added a silicone-covered palm, allowing the gripper to more closely resemble existing pneumatic grippers and to grasp with three or more points of contact.

Since our HSA pairs are made from PTFE, a very low friction material, we added various attachments to increase contact friction between the fingers and the grasped object. Each finger was wrapped in a thin (1/32") sheet of silicone, forming a glove. The glove was secured at the locked end of the HSA pair by a friction fit against the plastic cap. On the actuation end, the glove was secured to a plate between the gears and the HSA cylinders using a rubber band. The silicone glove expands as the HSA bends but does not slide off the ends. A 1/8" strip of neoprene foam was inserted between the PTFE tubes and the silicone glove to increase conformation of the finger to the object. The shape of the foam and the glove hold the foam pad in place against the HSA cylinders.

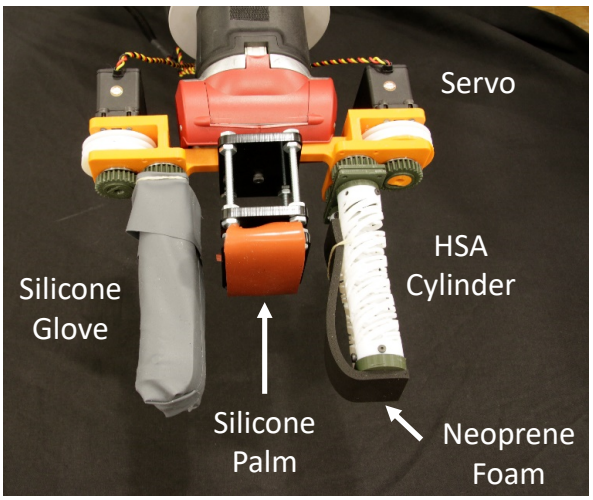

Fig. 7. A compliant hand made with two constrained handed shearing auxetic (HSA) pairs. On the left, we see the final finger, complete with silicone glove to enhance contact friction. On the right, we see the finger with the silicone glove removed, revealing the HSA pairs and the added foam to increase conformability to the grasped object.

VI. SOFT GRIPPER EVALUATION

To demonstrate the utility of our approach versus current pneumatic solutions, we directly compare our electrically-actuated gripper against a pneumatically-actuated soft gripper presented in [14]. To characterize both hands, we conduct experiments to evaluate (1) mechanical properties, (2) grasping success rate in a realistic application, and (3) gripper power consumption. A summary of evaluation metrics and results can be found in Table II.

The pneumatic hand utilized in this study had four fingers: one on the left side of the hand and three on the right. Each finger of the pneumatic gripper was actuated by a Concentric Glideforce LACT2P linear actuator controlled by a Pololu Jrk Motor Controller. Unlike the gripper first reported in [14], the pneumatic gripper used in this evaluation has added gecko-inspired adhesive patches [28], which significantly improve the static friction of the pneumatic hand. The evaluated pneumatic gripper also used the same silicone-covered palm as the HSA gripper rather than the original Ecoflex 00-10 silicone-based palm.

A. Mechanical Testing

Evaluating mechanical properties involved measuring static properties, such as finger and actuator dimensions, time to fabricate, radius of maximum finger curvature, and puncture resistance.

From the dimensions, we noted that although the HSA and pneumatic fingers were about the same size and had similar contact surface areas, the actuator system for the pneumatic hand is significantly larger and bulkier, a direct consequence of the need to translate electrical signals to airflow through large pressures. However, the HSA gripper had a radius of curvature that was twice as large as the pneumatic gripper. This is chiefly due to the difference in gripper material, as the pneumatic gripper's DragonSkin 20 is significantly more flexible than the PTFE used in the HSA system.

TABLE II
COMPARISON OF PNEUMATIC VS. HANDED SHEAR AUXETIC GRIPPERS

	Pneumatic	**Electric HSA**
Mechanical Properties		
Unactuated Finger Dimensions	120 mm x 27 mm x 20 mm	130 mm x 30 mm x 67 mm
Finger Weight	71.0 g	59.4 g
Actuator Dimensions	370 mm x 95 mm x 110 mm	50 mm x 28 mm x 58 mm
Actuator Weight	1160 g	105.8 g
Radius of Finger at Maximum Curvature	35 mm	75 mm
Approximate Fabrication Time	5.5 hr (silicone casting)	1.5 hr (laser cutting)
Puncture Resistance	Low	High
Grasping Tests		
Grasp Success Rate - Total	72%	72%
Grasp Success Rate - Regular Geometry	84%	80%
Grasp Success Rate - Irregular Geometry	54%	62%
Gripper Power Consumption		
Peak Power Usage	4.81 A @ 12 V	1.08 A @ 5V
Energy Required to Close Gripper	107.4 J $\pm$ 1.04 J	4.92 $\pm$ 0.23 J
Time to Close Gripper	2.90 $\pm$ 0.05 s	1.48 $\pm$ 0.05 s
Power Required to Maintain Closed State	1.21 $\pm$ 0.0023 W	5.32 $\pm$ 0.04 W
Energy Required to Open Gripper	93.5 $\pm$ 6.12 J	4.67 $\pm$ 0.22 J
Time to Open Gripper	2.82 $\pm$ 0.02 s	1.42 $\pm$ 0.04 s

The fabrication time for the pneumatic gripper was estimated to be about 5 hours; 4 hours for the DragonSkin 20A silicone to cure, 30 minutes for the DragonSkin 10A silicone to cure, and 30 minutes for assembly. The estimated fabrication time for the HSA gripper was 1.5 hour; 30 minutes to laser cut each PTFE tube, and 30 minutes for assembly. The time to create 3D printed parts was not included as these pieces could be reused, especially the 3D printed mold parts for the pneumatic gripper.

Evaluating puncture resistance was determined by using the relative surface area of each finger that could be punctured without immediate performance effects. For the pneumatic gripper, immediate pressure loss would occur if there was any hole puncturing one of the internal bladders. However, for punctures near the bladder, the weakened wall would deform differently than the surrounding area, possibly causing a bubble and rupture. For the HSA gripper, since there is no internal fluid, punctures do not materially affect gripper performance. A puncture would create a hole in the silicone glove surrounding the HSA cylinders and either pass through the HSA pattern harmlessly or hit an internal strut. While a perforated glove may reduce grasping performance by weakening the contact friction between the gripper and object, this is nowhere near as catastrophic as the pneumatic gripper's rupturing. Similarly, hitting an internal strut is unlikely to affect grasping performance as the compliance of the fingers will cause it to simply deflect from the puncture rather than break.

We do note that although the HSA gripper has high puncture resistance, it is susceptible to slicing cuts. Due to the many small features within the HSA pattern, a slice could potentially cut through key constraints or joints that the structure depends on. Further evaluation is needed on how many links within the HSA structure can be broken before system failure.

B. Grasping Tests

Grasping tests were conducted by mounting each hand to a Rethink Robotics Baxter robot and attempting to grasp a variety of common household groceries as well as objects from the YCB dataset [29]. The 32 objects selected can be seen in Fig. 8, and were chosen based on their wide range of material properties: large/small, regular/irregular geometries, heavy/light, and rigid/deformable. Since we were primarily interested in evaluating mechanical grasping performance, motion planning was not used to plan grasp orientation. Instead, objects were manually configured in an optimal orientation for each hand to ensure consistency and best possible performance of each grasp approach. In each experiment, the gripper would close on an object, attempt to lift the object, rotate the hand to ensure a tight stable grasp, and then return the object to its original location. Grasps were considered successful if an object remained grasped after arm translation and shaking.

The HSA gripper and pneumatic gripper had comparable performance; both were able to grasp 72% percent of the 32 tested objects (Fig. 8). The HSA gripper was better able to grasp small irregular objects (ex. diagonal cutters, broccoli), while the pneumatic gripper was better at grasping larger objects that it could envelop within its grasp (ex. wine bottle, fake banana). Both grippers had difficulty grasping heavy objects (ex. mustard bottle) and objects requiring a precision grasp style (ex. markers).

C. Gripper Power Consumption

To evaluate the efficiency of the system, we considered the total power consumption of the actuator to grasp a load. To measure power consumption, a DC power supply was directly connected to the gripper's actuators. The total current draw was then sampled through a single open/close movement, which was then analyzed for peak power usage as well as the energy required to open/close the gripper. For the pneumatic gripper, measurements of each of the four linear actuators were taken separately and then added together.

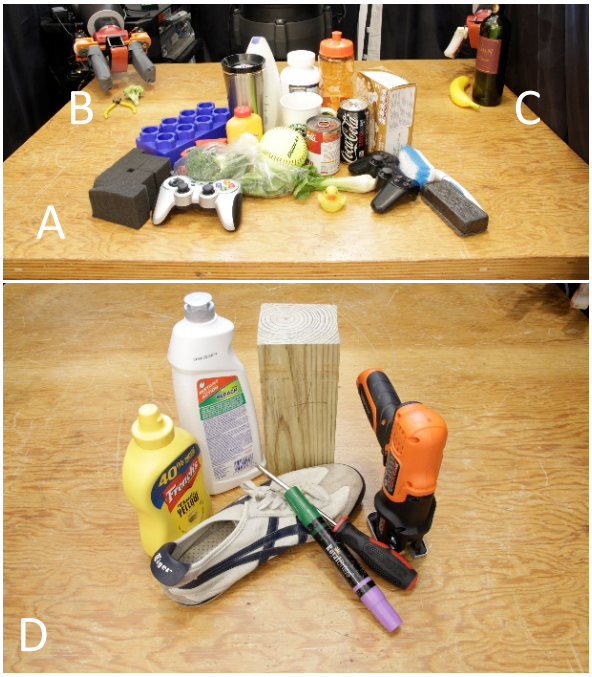

Fig. 8. Overall object set used for grasping experiments split up into (A) items grasped by both grippers, (B) items grasped by just the handed shearing auxetic gripper (broccoli, diagonal cutters), (C) items grasped by just the pneumatic gripper (wine bottle, fake banana) and (D) items grasped by neither grippers.

The HSA gripper was significantly faster and lower-power than the pneumatic system. The HSA gripper would open/close in half the time of the pneumatic gripper while also requiring nearly 20 times less energy. While the HSA gripper did require a higher amount of power to maintain a closed state, this could be mitigated by using a mechanism so that a closed state could be maintained without extra energy expenditure, such as the worm drive that is used in the pneumatic actuator's pump.

VII. CONCLUSIONS AND FUTURE WORK

This paper demonstrates the new and exciting potential of HSA-based actuators for soft robotics. By being elastically compliant, continuously deformable, and driven by electric motors, HSA-based actuators bridge the design space between series elastic actuators and soft robotics. Our mechanical characterization of the HSA cylinders has demonstrated comparable performance to other current soft actuation schemes – whether providing a useful range of motion as a linear actuator, demonstrating great flexibility when used for a 4-DOF platform, or grasping comparably well as a robotic gripper. The simplicity of HSA's actuation and fabrication scheme rivals that of pneunets in a form factor that is more puncture resistant, easier to interface with existing electrical systems, and more power efficient.

Future work will expand on these basic principles by creating new HSA patterns that can address more specific robotic applications. For example, although the current HSA cylinders are stiffer than current silicone actuators, making them less appropriate for extreme deformation contexts, using a different base material than PTFE for the HSA pattern may eliminate that issue. Likewise, a more optimized living hinge design within the HSA pattern may enable further extension for more applications. Further mechanical characterization is also needed to better understand how the compliance of the HSA cylinders change upon being extended as well as the optimal control scheme given this changing modulus.

ACKNOWLEDGMENTS

This work was done in the Distributed Robotics Laboratory at MIT with support from The Boeing Company and the National Science Foundation, grant numbers NSF IIS-1226883 and NSF CCF-1138967. The authors declare no competing financial interests.

REFERENCES

[1] D. Rus and M. T. Tolley, "Design, fabrication and control of soft robots," *Nature*, vol. 521, no. 7553, pp. 467–475, May 2015.

[2] Z.-W. Luo and M. Ito, "Control design of robot for compliant manipulation on dynamic environments," *IEEE Transactions on Robotics and Automation*, vol. 9, no. 3, pp. 286–296, 1993.

[3] G. A. Pratt and M. M. Williamson, "Series elastic actuators," in *Proceedings 1995 IEEE/RSJ International Conference on Intelligent Robots and Systems. Human Robot Interaction and Cooperative Robots*, vol. 1, Aug. 1995, pp. 399–406 vol.1.

[4] B. Mosadegh, P. Polygerinos, C. Keplinger, S. Wennstedt, R. F. Shepherd, U. Gupta, J. Shim, K. Bertoldi, C. J. Walsh, and G. M. Whitesides, "Pneumatic networks for soft robotics that actuate rapidly," *Advanced Functional Materials*, vol. 24, no. 15, pp. 2163–2170, 2014.

[5] S. Li, D. M. Vogt, D. Rus, and R. J. Wood, "Fluid-driven origami-inspired artificial muscles," *PNAS*, p. 201713450, Nov. 2017.

[6] M. A. Robertson and J. Paik, "New soft robots really suck: Vacuum-powered systems empower diverse capabilities," *Science Robotics*, vol. 2, no. 9, p. eaan6357, Aug. 2017.

[7] R. MacCurdy, R. Katzschmann, Y. Kim, and D. Rus, "Printable hydraulics: A method for fabricating robots by 3D co-printing solids and liquids," in *Robotics and Automation (ICRA), 2016 IEEE International Conference On*. IEEE, 2016, pp. 3878–3885.

[8] J. Hughes, U. Culha, F. Giardina, F. Guenther, A. Rosendo, and F. Iida, "Soft Manipulators and Grippers: A Review," *Frontiers in Robotics and AI*, vol. 3, Nov. 2016.

[9] P. Polygerinos, N. Correll, S. A. Morin, B. Mosadegh, C. D. Onal, K. Petersen, M. Cianchetti, M. T. Tolley, and R. F. Shepherd, "Soft robotics: Review of fluid-driven intrinsically soft devices; manufacturing, sensing, control, and applications in human-robot interaction," *Advanced Engineering Materials*.

[10] C. Laschi, B. Mazzolai, and M. Cianchetti, "Soft robotics: Technologies and systems pushing the boundaries of robot abilities," *Science Robotics*, vol. 1, no. 1, p. eaah3690, 2016.

[11] M. Wehner, M. T. Tolley, Y. Mengüç, Y.-L. Park, A. Mozeika, Y. Ding, C. Onal, R. F. Shepherd, G. M. Whitesides, and R. J. Wood, "Pneumatic energy sources for autonomous and wearable soft robotics," *Soft Robotics*, vol. 1, no. 4, pp. 263–274, 2014.

[12] R. F. Shepherd, A. A. Stokes, R. M. D. Nunes, and G. M. Whitesides, "Soft Machines That are Resistant to Puncture and That Self Seal," *Advanced Materials*, vol. 25, no. 46, pp. 6709–6713, Dec. 2013.

[13] A. D. Marchese, C. D. Onal, and D. Rus, "Soft robot actuators using energy-efficient valves controlled by electropermanent magnets," in *Intelligent Robots and Systems (IROS), 2011 IEEE/RSJ International Conference On*. IEEE, 2011, pp. 756–761.

[14] B. S. Homberg, R. K. Katzschmann, M. R. Dogar, and D. Rus, "Haptic identification of objects using a modular soft robotic gripper," in *Intelligent Robots and Systems (IROS), 2015 IEEE/RSJ International Conference On*. IEEE, 2015, pp. 1698–1705.

[15] K. C. Galloway, P. Polygerinos, C. J. Walsh, and R. J. Wood, "Mechanically programmable bend radius for fiber-reinforced soft actuators," in *Advanced Robotics (ICAR), 2013 16th International Conference on*. IEEE, 2013, pp. 1–6.

[16] B. Mazzolai, L. Margheri, M. Cianchetti, P. Dario, and C. Laschi, "Soft-robotic arm inspired by the octopus: II. From artificial requirements to innovative technological solutions," *Bioinspiration & Biomimetics*, vol. 7, no. 2, p. 025005, June 2012.

[17] A. S. Boxerbaum, K. M. Shaw, H. J. Chiel, and R. D. Quinn, "Continuous wave peristaltic motion in a robot," *The international journal of Robotics Research*, vol. 31, no. 3, pp. 302–318, 2012.

[18] J. M. Bern, G. Kumagai, and S. Coros, "Fabrication, modeling, and control of plush robots," in *Proceedings of the International Conference on Intelligent Robots and Systems*, 2017.

[19] D. Paluska and H. Herr, "The effect of series elasticity on actuator power and work output: Implications for robotic and prosthetic joint design," *Robotics and Autonomous Systems*, vol. 54, no. 8, pp. 667–673, Aug. 2006.

[20] J. N. Grima, P.-S. Farrugia, R. Gatt, and D. Attard, "On the auxetic properties of rotating rhombi and parallelograms: a preliminary investigation," *physica status solidi (b)*, vol. 245, no. 3, pp. 521–529, 2008.

[21] C. Borcea and I. Streinu, "Geometric auxetics," in *Proc. R. Soc. A*, vol. 471, no. 2184. The Royal Society, 2015, p. 20150033.

[22] A. Yeganeh-Haeri, D. J. Weidner, and J. B. Parise, "Elasticity of α-cristobalite: A silicon dioxide with a negative poisson's ratio," *Science*, vol. 257, no. 5070, pp. 650–652, 1992.

[23] R. H. Baughman, J. M. Shacklette, A. A. Zakhidov, and S. Stafström, "Negative poisson's ratios as a common feature of cubic metals," *Nature*, vol. 392, no. 6674, pp. 362–365, 1998.

[24] R. Lakes, "Foam structures with a negative poisson's ratio," *Science*, vol. 235, pp. 1038–1041, 1987.

[25] J. N. Grima, E. Chetcuti, E. Manicaro, D. Attard, M. Camilleri, R. Gatt, and K. E. Evans, "On the auxetic properties of generic rotating rigid triangles," in *Proc. R. Soc. A*. The Royal Society, 2011, p. rspa20110273.

[26] J. I. Lipton, R. MacCurdy, Z. Manchester, L. Chin, D. Celluci, and D. Rus, "Handedness in Shearing Auxetics Creates Rigid and Compliant Structures," *Science*, (2018, in press).

[27] W. Felt and C. D. Remy, "A closed-form kinematic model for fiber-reinforced elastomeric enclosures," *Journal of Mechanisms and Robotics*, vol. 10, no. 1, p. 014501, 2018.

[28] E. W. Hawkes, E. V. Eason, D. L. Christensen, and M. R. Cutkosky, "Human climbing with efficiently scaled gecko-inspired dry adhesives," *Journal of The Royal Society Interface*, vol. 12, no. 102, p. 20140675, 2015.

[29] B. Calli, A. Singh, J. Bruce, A. Walsman, K. Konolige, S. Srinivasa, P. Abbeel, and A. M. Dollar, "Yale-CMU-Berkeley dataset for robotic manipulation research," *The International Journal of Robotics Research*, vol. 36, no. 3, pp. 261–268, Mar. 2017.